Mathematical and Computational Applications

MDPI

Article

A Strain-Gauge-Based Method for the Compensation of Out-of-Plane Motions in 2D Digital Image Correlation

Carl-Hein Visser , Gerhard Venter * and Melody Neaves

Department of Mechanical and Mechatronic Engineering, Stellenbosch University, Private Bag X1, Matieland 7602, South Africa

* Correspondence: gventer@sun.ac.za

Abstract: When performing a digital image correlation (DIC) measurement, multi-camera stereo-DIC is generally preferred over single-camera 2D-DIC. Unlike 2D-DIC, stereo-DIC is able to minimise the in-plane strain error that results from out-of-plane motion. This makes 2D-DIC a less viable alternative for strain measurements than stereo-DIC, despite being less financially and computationally expensive. This work, therefore, proposes a strain-gauge-based method for the compensation of errors from out-of-plane motion in 2D-DIC strain measurements on planar specimens. The method was first developed using equations for the theoretical strain error from out-of-plane motions in 2D-DIC and was then applied experimentally in tensile tests to two different dog-bone specimen geometries. The compensation method resulted in a clear reduction in the strain error in 2D-DIC. The strain-gauge-based method thus improves the accuracy of a 2D-DIC measurement, making it a more viable option for performing full-field strain measurements and providing a possible alternative in cases where stereo-DIC is not practical or is unavailable.

Keywords: digital image correlation; error compensation; out-of-plane motion; strain gauges; full-field strain data

Citation: Visser, C.-H.; Venter, G.; Neaves, M. A Strain-Gauge-Based Method for the Compensation of Out-of-Plane Motions in 2D Digital Image Correlation. *Math. Comput. Appl.* **2023**, *28*, 40. https://doi.org/10.3390/mca28020040

Academic Editors: Hans Beushausen and Sebastian Skatulla

Received: 15 February 2023
Revised: 6 March 2023
Accepted: 8 March 2023
Published: 10 March 2023

1. Introduction

Digital image correlation (DIC) is an optical metrology tool used to measure full-field surface deformations. A correlation algorithm is used in DIC to process images taken of a test specimen while being deformed. The algorithm tracks the motion of a subset of the image, before and after deformation. From this, quantities-of-interest, such as displacement and strain, can then be measured using DIC. Importantly, to use the DIC algorithm, a test specimen should have a speckle pattern on its surface before testing. This may occur naturally on the specimen's surface or may be applied to it. Since its inception in the 1980s by Peters and Ranson [1], DIC has been applied in a wide variety of structural and material engineering contexts. Some of the examples which demonstrates DIC's versatility include: determining the material properties of brain tissue [2], lifetime assessment of steam pipelines in coal-fired power plants [3] and using scanning electron microscope (SEM) imaging and DIC to perform micro-scale deformation measurements [4]. The popularity of DIC can largely be attributed to factors [5] such as the relative simplicity of using DIC (compared to similar non-contact measurement tools) and its flexible and extensive measurement sensitivity and resolution. It also has less strict prerequisites for its test setup compared to other non-contact measurement tools.

When performing DIC, it can either be carried out as 2D-DIC, which uses a single-camera setup, or as stereo-DIC, which uses a multi-camera setup to implement stereo-vision. When DIC is performed, it is typically in the form of stereo-DIC due to the inherent displacement and strain measurement accuracy of stereo-DIC relative to 2D-DIC. Even though stereo-DIC is more accurate than 2D-DIC, 2D-DIC has the benefits of being less expensive in terms of both its hardware and software costs, and also in terms of its computational overhead [6]. 2D-DIC also has less strict testing requirements than stereo-DIC, as stereo-DIC, for example, requires a camera calibration procedure to be performed to relate the camera positions relative to one another. 2D-DIC, though, only requires its measurements to be linearly scaled from pixel to real-world coordinates [6]. Therefore, if the accuracy of 2D-DIC is improved, it would provide a suitable low-cost alternative to stereo-DIC.

To improve the accuracy of 2D-DIC, two main error sources namely lens distortions and out-of-plane motions, should be addressed. While the errors from lens distortions are significant, various compensation methods for this error are readily available [7], e.g., the camera calibration procedure. Unlike with lens distortions, there is not a simple or readily available method of compensating for errors from out-of-plane motions. Out-of-plane motions exist in two main forms: the non-perpendicularity of the camera's optical axis relative to the specimen's surface and the out-of-plane motion of the specimen relative to the camera (or the camera relative to the specimen). Both forms of out-of-plane motions are common in mechanical testing, such as in tensile testing, and are difficult to avoid. Out-of plane translations and rotations can, for example, occur from a non-planar test specimen, the test specimen bending during testing, the contraction of the specimen due to Poisson's effect, the specimen expanding from heating during testing, the specimen necking while being loaded, and the specimen not being ideally clamped by its grips [8].

It is important to consider some of the correction methods which have been developed before, as they each have their respective advantages and disadvantages. A notable 2D-DIC error correction method is the Region of Compensation method. It was originally proposed by Pan et al. [9], and was then validated by Wittevrongel et al. [10] and further improved upon by Xu et al. [11]. This method uses a compensation panel which is rigidly attached to the test specimen to correct for displacement and strain errors in a 2D-DIC measurement and is able to compensate for errors from both lens distortions and out-of-plane motions. It is limited by the fact that it alters the test specimen and that it involves the post-processing of measured data. The method also makes various assumptions on the behaviour of the compensation panel during testing and it also can only be used in test cases where the compensation panel can be attached to the specimen. Another compensation method is the Image Rectification method which was first proposed by Lava et al. [12]. Later modifications on the method were then proposed by both Wittevrongel et al. [10] and Hijazi [6]. Their method numerically transforms the image captured during a DIC test to appear as though they have been captured by a perpendicular camera setup. The effect of any non-perpendicularity in the camera setup (relative to the specimen) is thus removed from the measurement. The benefits of this method is that no additional hardware is needed and that it compensates for errors both from camera non-perpendicularity and from lens distortions. The limitations of this method is that the data is pre-processed and that any out-of-plane motions which may occur during the test are not corrected for. Using a bilateral telecentric lens (instead of a standard lens) to compensate for errors from out-of-plane motions is another method. This compensation method was initially proposed by Sutton et al. [8] as bilateral telecentric lenses are insensitive to out-of-plane motions and capture images at a constant magnification [13]. Replacing a standard lens in a 2D-DIC test setup with a bilateral telecentric lens is likely the simplest method to compensate for errors from out-of-plane motions. However, a bilateral telecentric lens is limited by its fixed magnification and field-of-view, as well as its restricted depth-of-focus. Bilateral telecentric lenses are also significantly more expensive than standard lenses, with the cost of some bilateral telecentric lenses being about ten times that of a standard lens [13].

A compensation method is thus proposed which corrects for strain errors from out-of-plane motion in 2D-DIC measurements, on planar specimens, using strain gauge measurement data. The method is first developed using equations derived for the theoretical strain errors in 2D-DIC data from out-of-plane translations and rotations. The method is then applied to test specimens that are loaded in tension. Stereo-DIC, 2D-DIC and strain gauge measurements are taken simultaneously throughout the test, where stereo-DIC is captured as a reference measurement. Two types of specimens were tested: a simple dog-bone specimen, which produces a homogeneous strain field, and a dog-bone specimen, with two holes and a slot, which produces a heterogeneous strain field. Both specimens had a speckle pattern on their front surface and strain gauges applied to their back surface. This method leads to a clear improvement in the accuracy of 2D-DIC measurements and is relatively easy to use and relatively low-cost (if a low-cost data acquisition system is used). The improvement in the accuracy of the 2D-DIC data from this method makes using 2D-DIC a more viable option for performing full-field surface deformation measurements. The corrected 2D-DIC thereby offers an alternative to stereo-DIC in situations where it may be unavailable due to test setup or financial constraints.

2. Materials and Methods

2.1. Development of the Strain-Gauge-Based Error Compensation Method

The proposed error compensation method was developed by first analysing the theoretical error in 2D-DIC data resulting from out-of-plane motion. For this, equations were derived for the strain theoretical error from the two main types of out-of-plane motion: out-of-plane translation of a flat plane and out-of-plane rotation of a flat plane. From there, a simplified equation with three unknown coefficients, was obtained. If the unknown coefficients can be found, then this equation is able to describe the theoretical total strain error from out-of-plane motion present in the full-field 2D-DIC data. Using strain gauge measurements as the ground truth is proposed to find the strain error from out-of-plane motion in a 2D-DIC measurement, by solving for the unknown coefficients. With the total strain error equation known, the strain over the entire strain field can be corrected by subtracting the error estimated from this equation from the measured strain values.

2.1.1. Theoretical Error from Out-of-Plane Motion in 2D-DIC

The equations for the out-of-plane motion error were derived using the idealised pinhole imaging model, shown in Figure 1.

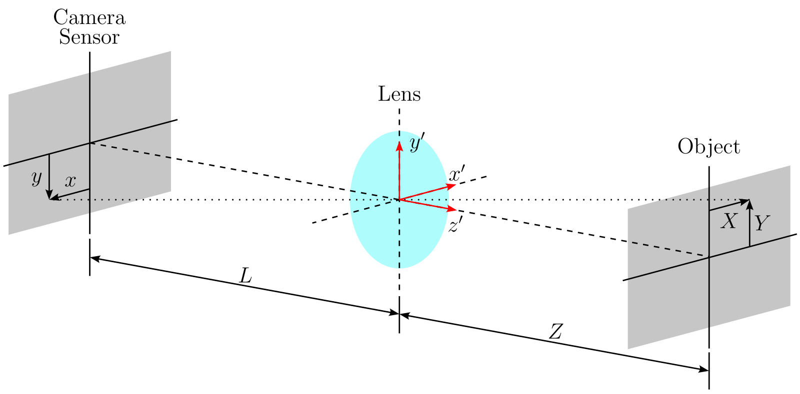

Figure 1. A 3D depiction of the pinhole imaging model [14].

From the pinhole imaging model, the object dimensions X and Y are each related to their corresponding image dimensions x and y, where L is the image distance and Z is the object distance. To obtain the theoretical strain errors due to out-of-plane motion, the change in the image dimensions from the out-of-plane motion were first derived. This change resulted in the artificial in-plane displacements U and V, which in turn produced the erroneous in-plane strain fields of ε_{xx} and ε_{yy}. These derivations were performed in the y'-z' plane, using the coordinate system defined in Figure 1, and resulted in the following equations:

- **Out-Of-Plane Translation:** Object out-of-plane translation ΔZ results in the in-plane strain errors ε_{xx} and ε_{yy} as follows [8]:

$$\varepsilon_{xx}(\Delta Z) = \frac{\delta U(\Delta Z)}{\delta x} = -\frac{\Delta Z}{Z} \tag{1}$$

$$\varepsilon_{yy}(\Delta Z) = \frac{\delta V(\Delta Z)}{\delta y} = -\frac{\Delta Z}{Z} \tag{2}$$

- **Out-Of-Plane Rotation:** Object out-of-plane rotation θ about the horizontal measurement axis (which is the X-axis in this case) results in in-plane strain errors ε_{xx} and ε_{yy} as follows [8]:

$$\varepsilon_{xx}(\Delta Z) = \frac{\delta U(\Delta Z)}{\delta x} = -\frac{Y \sin\theta}{Z} \tag{3}$$

$$\varepsilon_{yy}(\Delta Z) = \frac{\delta V(\Delta Z)}{\delta y} = \cos\theta - 1 - \frac{2Y\cos\theta\sin\theta}{Z} = \cos\theta - 1 - \frac{Y\sin 2\theta}{Z} \tag{4}$$

The effect of out-of-plane translation and rotation in the x'-z' plane would produce similar equations to Equations (1)–(4). For further detail, readers are encouraged to refer to the full derivations of the in-plane strain error equations resulting from out-of-plane motion in [8].

2.1.2. Simplified Equation for the Total Error from Out-of-Plane Motion

From the analysis of the various cases of out-of-plane motion and their corresponding strain error equations, a single, simplified equation was obtained which represents the total strain error from out-of-plane motion. For this, the various ways in which out-of-plane motion would present itself during a DIC measurement was first analysed. The possible scenarios of out-of-plane motions and their respective strain error equations, which are also shown in Figure 2, were found to be:

1. Translation perpendicular to the measurement plane (from Equation (2)):

$$\varepsilon_{yy,\ error}(\Delta Z_i) = -\frac{\Delta Z_i}{Z} \tag{5}$$

2. Rotation about the horizontal (in-plane) measurement axis (from Equation (4)):

$$\varepsilon_{yy,\ error}(Y, \theta_i) = \cos\theta_i - 1 - \frac{Y\sin 2\theta_i}{Z} \tag{6}$$

3. Rotation about the vertical (in-plane) measurement axis (from the result of performing the same derivation as for Equation (4), but around the vertical axis instead):

$$\varepsilon_{yy,\ error}(X, \phi_i) = \frac{X\sin\phi_i}{Z} \tag{7}$$

where ΔZ_i, θ_i and ϕ_i are the i-th points of ΔZ, θ and ϕ, i.e., at time t_i. The strain error equations have been given as functions of their instantaneous out-of-plane motion values, as the out-of-plane motions would likely be varying with time, i.e., throughout the measurement. Rotation about the z-axis was not considered here as the 2D-DIC algorithm is made to measure both in-plane translations and rotations, and as long as the in-plane rotation is relatively small, then it should not present any problems to the measurement ability of 2D-DIC [5,10].

Since Equations (5)–(7) are given in terms of instantaneous variables, when a single moment in time (during a DIC measurement) is considered, then each of the coefficients in these equations can be represented by a single constant. This allows the strain error equations to be simplified as:

1. Translation perpendicular to the measurement plane (from Equation (5)):

$$\varepsilon_{yy,\ error} = a_{0,i} \tag{8}$$

2. Rotation about the horizontal (in-plane) measurement axis (from Equation (6)):

$$\varepsilon_{yy,\ error}(Y) = a_{1,i} + a_{2,i}Y \tag{9}$$

3. Rotation about the vertical (in-plane) measurement axis (from Equation (7)):

$$\varepsilon_{yy,\ error}(X) = a_{3,i}X \tag{10}$$

Finally, a single equation, which represents the combined effect of all three cases of out-of-plane motion, is obtained from the superposition of the three simplified strain error equations (Equations (8)–(10)):

$$\begin{aligned}\varepsilon_{yy,\ total\ error}(X,Y) &= a_{0,i} + a_{1,i} + a_{2,i}Y + a_{3,i}X \\ &= A_i + B_iY + C_iX\end{aligned} \tag{11}$$

When out-of-plane motion occurs, it causes a strain error over the entire full-field measured by 2D-DIC, and so Equation (11) describes the theoretical total error from out-of-plane motion over the entire area being measured.

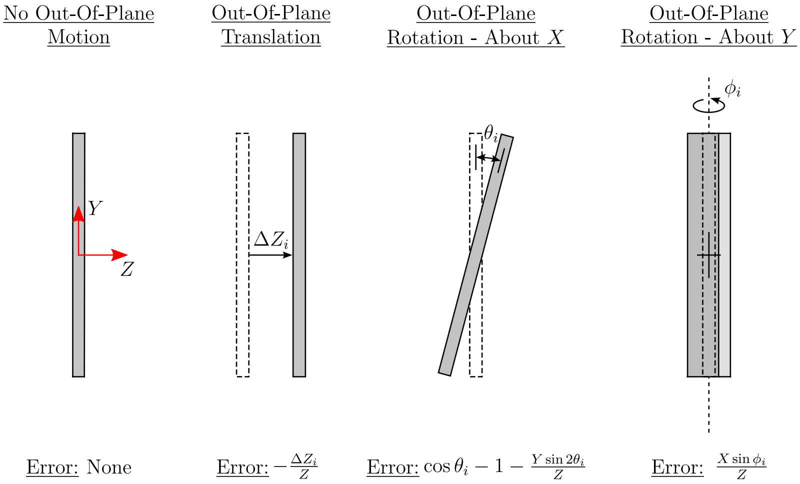

Figure 2. The possible forms of out-of-plane motion which can occur during a test and the corresponding equations which describe their strain errors.

2.1.3. Compensation of Error from Out-of-Plane Motion

The error from out-of-plane motion in the 2D-DIC measurement would be compensated for by removing the results from Equation (11) from the strain measurement as it represents the total strain error from out-of-plane motion in 2D-DIC data. To achieve this, the three unknown coefficients in Equation (11) must firstly be solved for using (a minimum of) three known strain error values and their respective X and Y positions. Strain gauges are proposed as the ground truth for calculating the strain error values as they provide a simple, effective way of obtaining accurate strain values at discrete locations. The strain error values can then be calculated as:

$$\varepsilon_{yy,\ total\ error-n} = \varepsilon_{yy,\ DIC-n} - \varepsilon_{yy,\ SG-n} \tag{12}$$

where $\varepsilon_{yy,\ total\ error-n}$ is total strain error in the 2D-DIC measurement, $\varepsilon_{yy,\ DIC-n}$ is the strain extracted from the 2D-DIC data by a virtual strain gauge and $\varepsilon_{yy,\ SG-n}$ is the strain measured by a strain gauge, all for the same location n. To solve for the unknown coefficients, a system of linear equations is set up using Equation (11) and is solved as in Equation (13):

$$\begin{bmatrix} 1 & Y_1 & X_1 \\ 1 & Y_2 & X_2 \\ 1 & Y_3 & X_3 \end{bmatrix} \begin{bmatrix} A \\ B \\ C \end{bmatrix} = \begin{bmatrix} \varepsilon_{yy,\ total\ error\ 1} \\ \varepsilon_{yy,\ total\ error\ 2} \\ \varepsilon_{yy,\ total\ error\ 3} \end{bmatrix} \tag{13}$$

A more accurate fit can also be achieved by using more than three datapoints and then performing a least-squares fit of the data, as in Equation (14):

$$\begin{bmatrix} 1 & Y_1 & X_1 \\ 1 & Y_2 & X_2 \\ \vdots & \vdots & \vdots \\ 1 & Y_n & X_n \end{bmatrix} \begin{bmatrix} A \\ B \\ C \end{bmatrix} = \begin{bmatrix} \varepsilon_{yy,\ total\ error\ 1} \\ \varepsilon_{yy,\ total\ error\ 2} \\ \vdots \\ \varepsilon_{yy,\ total\ error\ n} \end{bmatrix} \tag{14}$$

where n is the number of strain gauges. With the unknown coefficients found, Equation (11) can be used to estimate the strain error over the entire field of 2D-DIC data. The strain error can now be compensated for by simply subtracting it from the full-field 2D-DIC strain data to produce corrected 2D-DIC strain data. This process is repeated at each time-step in the 2D-DIC measurement so that the error from out-of-plane motion throughout the entire measurement is corrected.

2.2. *Experimental Application of Strain Gauge Error Compensation Method*

The error compensation method was applied to two experiments to practically verify its functionality. A tensile test was performed on two different dog-bone specimens, where the specimen's strain was measured using stereo-DIC, 2D-DIC and strain gauges simultaneously.

2.2.1. Test Setup

The test setup for the verification experiment is shown in Figure 3 and consists of: a tensile test machine, a stereo-DIC measurement setup for performing both stereo-DIC and 2D-DIC, and a bridge amplifier for the strain gauge measurements. A single stereo-DIC setup could be used to perform both stereo-DIC and 2D-DIC measurements as it had an asymmetric stereo-angle between the two DIC cameras [11]. With this setup, one of the cameras was approximately perpendicular to the test specimen, for performing 2D-DIC, while the other camera was at a stereo-angle of approximately 20°, for performing a stereo-DIC measurement using both cameras. A stereo-DIC measurement was performed as a reference measurement to compare the corrected 2D-DIC measurement against.

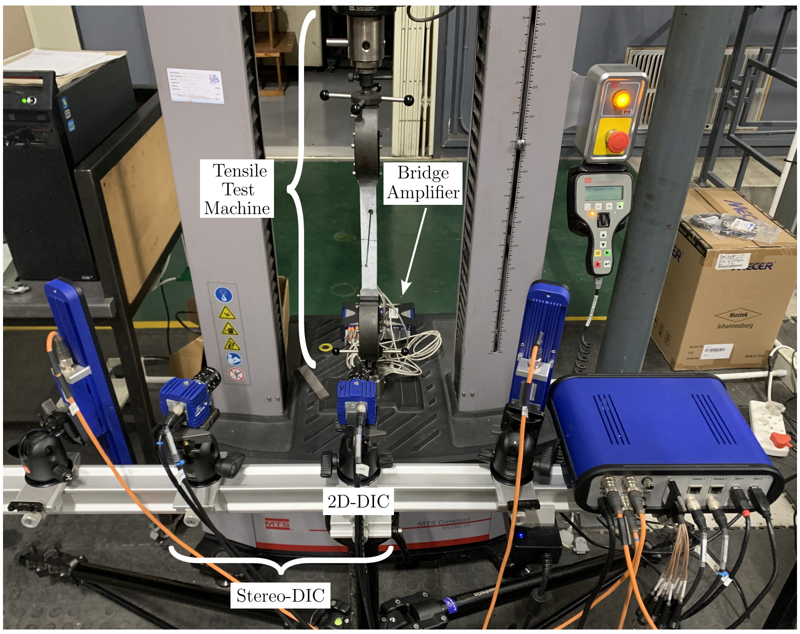

Figure 3. Test setup used for the experimental verification of the strain-gauge-based error compensation method.

The details of the DIC hardware used in the verification experiments is summarised in Table 1.

Table 1. Hardware parameters for the DIC setup. Parameters were the same for both tests, except where stated to be different.

Cameras	LaVision Imager M-lite 5M
Image resolution	2464 × 2056 pixels^2
Lenses	RICOH FL-CC3516-2M TV LENS
Focal length	35 mm
Field-of-view	Simple specimen tests: 90.7 × 108.8 mm^2; Complex specimen tests: 121.7 × 145.8 mm^2
Image scale	Simple specimen tests: 23.3 pixels/mm; Complex specimen tests: 17.3 pixels/mm
Stand-off distance	Simple specimen tests: 430.85 mm; Complex specimen tests: 654.58 mm
Image acquisition rate	10 Hz
Lighting	White linear LED arrays
Aperture	Simple specimen tests: f/4.5; Complex specimen tests: f/7
Patterning method	Matte white spray painted-base coat, matte black spray painted-speckles
Approximate pattern feature size (major diameter)	Simple specimen tests: 3–21 pixels (0.13–0.90 mm); Complex specimen tests: 3–30 pixels (0.17–1.73 mm)

2.2.2. Test Specimens

Two different dog-bone specimen geometries were designed for the experimental application of the error compensation method. The first “simple” test specimen is a dog-bone shaped tensile test specimen designed according to the specifications for a sheet-type rectangular-shaped tensile test specimens in the ASTM E8/E8M standard [15] and is shown in Figure 4. It was designed to be an ideal case for measuring strain with 2D-DIC, as relatively little out-of-plane motion is expected from the specimen and, therefore, the strain errors in the measurement would likely also be low. The second “complex” test specimen, shown in Figures 5, is also a dog-bone test specimen, but with two holes and a slot cut from it. It was also initially designed using the ASTM E8/E8M standard, but was made thinner due to manufacturing constraints. The two holes and slot were added to the specimen design so that the specimen produces a heterogeneous strain field while it is loaded, and thus provides an example which the error compensation method can be demonstrated on for a complex strain field. This specimen is also expected to experience more out-of-plane motions that the simple specimen, due to its complex geometry, thus providing a non-ideal case for 2D-DIC strain measurements. Both of the specimen geometries were manufactured from Aluminium Alloy 1050A. The specimens were prepared with a speckle pattern on its front, as is required for DIC measurement, with markings made on the speckle pattern to serve as a common origin for the real-world and DIC coordinate systems. The specimens also have a set of strain gauges on the back, where the simple specimen had three strain gauges applied to it and the complex specimen had four strain gauges applied to it, as depicted in Figures 4 and 5. The locations of the strain gauges were selected to be far enough away from stress concentrations and to cover a large footprint over the surface area being measured.

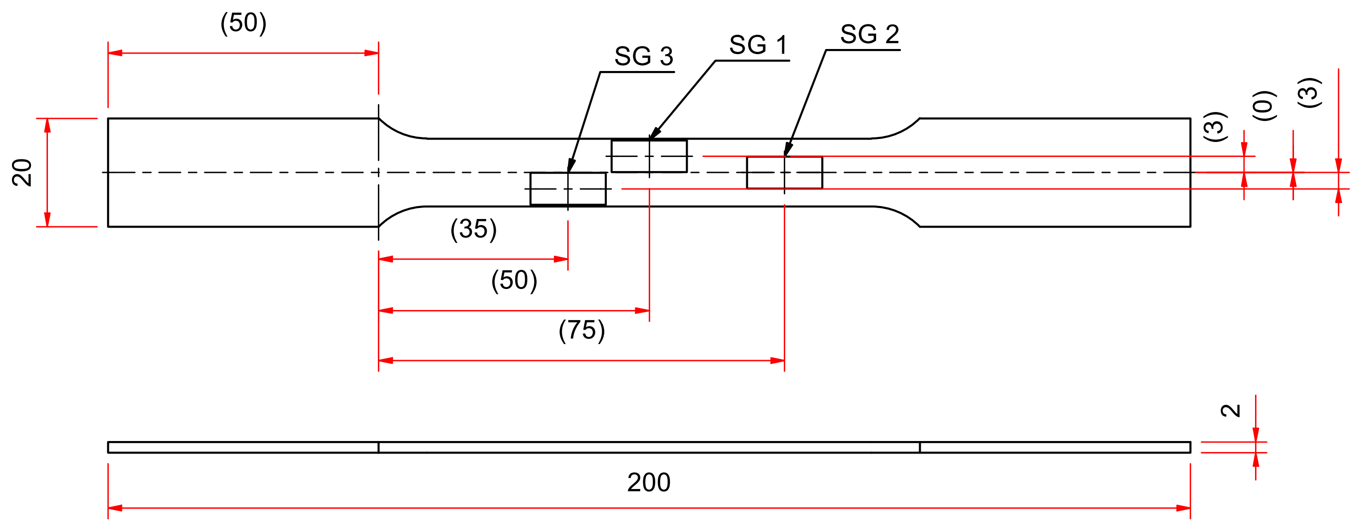

Figure 4. Schematic of the simple test specimen and the locations and naming conventions of strain gauges. Dimensions are in millimetres.

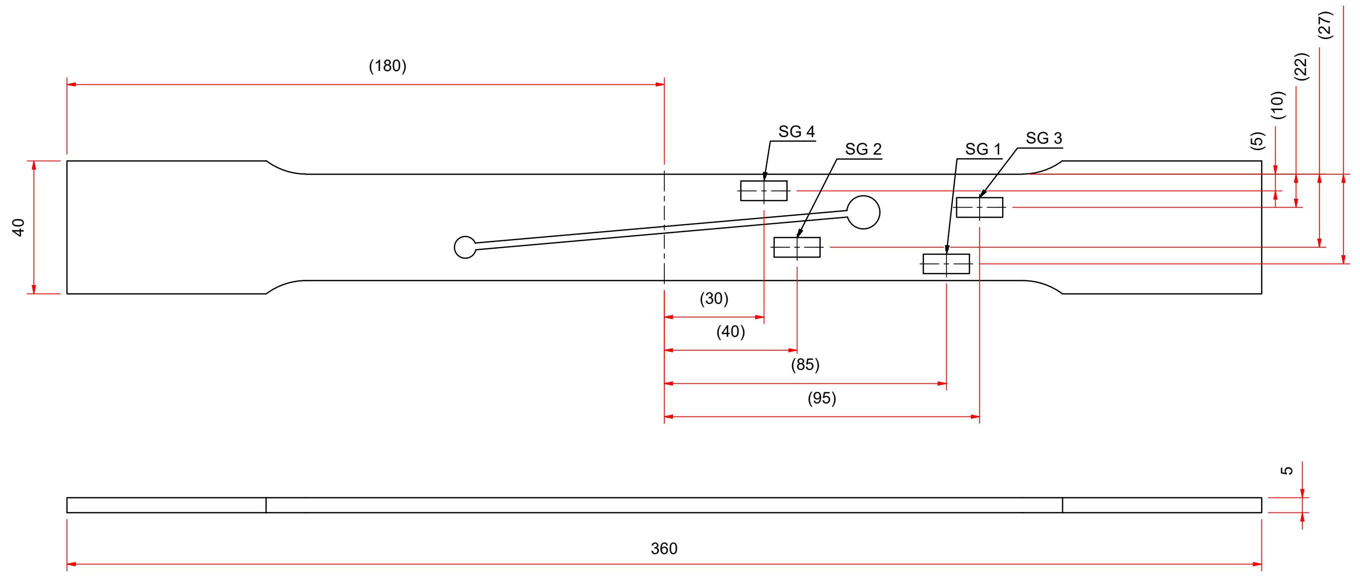

Figure 5. Schematic of the complex test specimen and the locations and naming conventions of strain gauges. Dimensions are in millimetres.

2.2.3. Experimental Procedure

A similar experimental procedure was followed for both sets of tests for the two different specimen geometries. In both sets of tests, 2D-DIC, stereo-DIC and strain gauge measurements were performed simultaneously. The strain gauge data could simply be stored after being measured, although both the images taken for 2D-DIC and stereo-DIC first had to be processed using LaVision DaVis 10.2.1 before their respective strain measurements could be extracted. The parameters used in the processing of the DIC measurements is listed in Table 2. The main difference in the procedures followed between the two sets of test was the force to which the different specimens were loaded. Specifically that:

- **Simple specimen tests**: The specimen was only loaded to approximately half of the specimen material's yield strength. This allows multiple tensile tests to be conducted on the same specimen within the elastic range of the specimen. In this manner, other experimental variables (for example, different speckle patterns and setup conditions) can be eliminated.

- **Complex specimen tests**: The specimens were loaded to past the ultimate strength of the specimen (where parts of the specimen had begun necking). The complex specimens were at first also loaded to only half of their material's yield strength, so that the same specimen could be tested more than once, as in the simple specimen tests. To avoid exceeding half the yield strength anywhere in the specimen, the specimens were loaded to a force which resulted in a stress of half the yield strength at the stress concentrations. At this force, the rest of the specimen experienced very low strains, which were close to the 2D-DIC noise floor of the experiment. This made the DIC strain data very noisy and caused inaccuracies in the strain errors calculated between the 2D-DIC and strain gauge data. This meant that a fit of the strain errors (as in Equation (13)) would not accurately describe the strain error in the full-field 2D-DIC data, and so the error compensation method could not successfully be applied. A different specimen was, therefore, used in each of the tests and was loaded to above its yield strength so that high strains were induced across the whole strain field.

After all the specimens were tested and the DIC data was processed, the measured data was imported into a Python script which applied the error compensation method to the data and produced corrected 2D-DIC data.

Table 2. Parameters used in the DIC analysis. Parameters were the same for both tests, except where stated to be different.

Software	LaVision DaVis 10.2.1
Subset size	Simple specimen tests: 61 pixels (2.62 mm); Complex specimen tests: 61 pixels (3.53 mm)
Step size	Simple specimen tests: 20 pixels (0.86 mm); Complex specimen tests: 20 pixels (1.16 mm)
Subset shape function	Affine
Strain formulation	Engineering strain
Virtual strain gauge size	Simple specimen tests: 139.8×65.24 pixels^2 (6×2.8 mm^2) [1]; Complex specimen tests: 103.8×48.44 pixels^2 (6×2.8 mm^2) [1]
Strain noise floor	Simple specimen tests: stereo-DIC—41.3 µmm/mm, 2D-DIC—39.6 µmm/mm; Complex specimen tests: stereo-DIC—47.6 µmm/mm, 2D-DIC—30.6 µmm/mm
Strain bias	Simple specimen tests: stereo-DIC—3.6 µmm/mm, 2D-DIC—9.3 µmm/mm; Complex specimen tests: stereo-DIC—−2.1 µmm/mm, 2D-DIC—−1.7 µmm/mm
Out-of-plane motion strain bias	Simple specimen tests: 1972 µmm/mm per mm; Complex specimen tests: 1535 µmm/mm per mm

[1] The physical size of the virtual strain gauges used was the same for both experiments as they were made to be the same size as the strain gauges used during the experiments.

3. Results

A set of tensile tests were conducted on each of the specimens shown in Figures 4 and 5. Five and three tensile tests were conducted on the simple and complex specimens, respectively. Stereo-DIC data is captured simultaneously along with 2D-DIC and strain gauge as it serves as a reference measurement which the 2D-DIC plots, before and after compensation, can be compared against. The plots have all been carried out for the strain measured in the y-direction, which is aligned with the direction that the specimen was loaded in during testing.

3.1. Simple Tensile Specimen Tests

From the tests conducted on the simple specimen geometry, none of the five tests showed a significant improvement in the strain measurement accuracy, with an example of the results from one of the tests shown in Figure 6. The plots labelled as "2D-DIC" and "Corrected 2D-DIC" show the 2D-DIC data before and after the error compensation method was applied to it, respectively. Similarly, the plots labelled as "|Error| Before Correction" and "|Error| After Correction" respectively show the absolute error difference between the stereo-DIC and 2D-DIC measurements, before and after the compensation method was used on the 2D-DIC data.

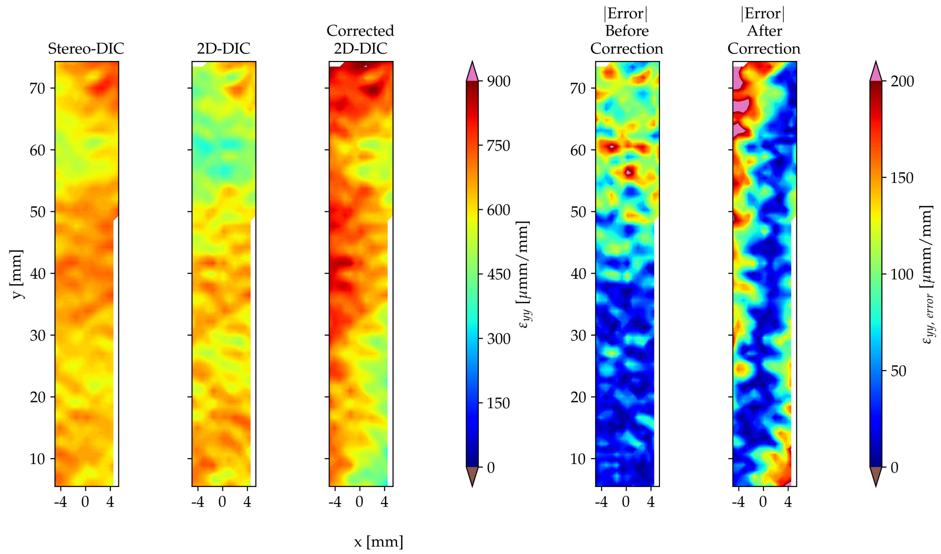

Figure 6. Results from the application of the compensation method to the 2D-DIC measurement taken in Test 4, for the last image taken in the tensile test.

The root-mean-square (RMS) error of all strain measurements across the region-of-interest before and after correction during Test 4 is shown in Figure 7. This illustrates how the measurement accuracy throughout the whole measurement remains relatively the same after applying the error compensation, which was similar in all of the tests conducted.

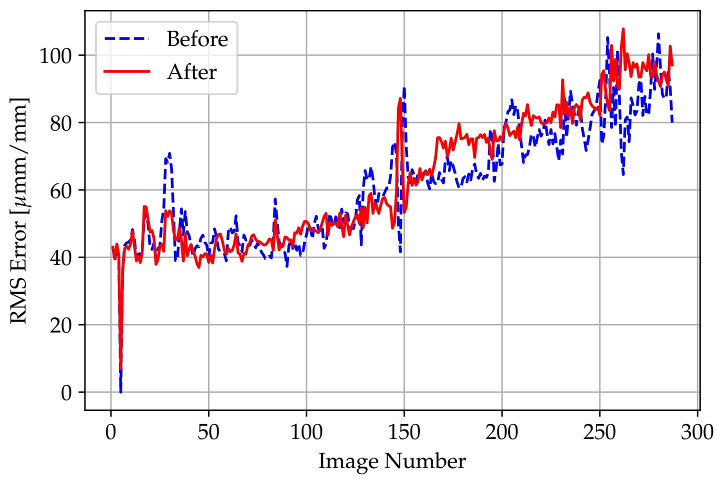

Figure 7. RMS error difference between stereo-DIC and 2D-DIC before and after correction for Test 4.

The main reason why the accuracy did not significantly improve in these tests can be attributed to the fact that the specimens experienced relatively little out-of-plane motion, as shown in Figure 8. Because of this, the 2D-DIC performs relatively on par with stereo-DIC and leads to a strain error (before correction) which is on the order of magnitude of the noise-floor (about 40 µmm/mm) for this experiment, as shown in Figure 6. Since the strain error was so close to the noise-floor already, there was a negligible amount bias error which could be corrected for, leading to the accuracy of the 2D-DIC measurements being relatively the same after correction as before correction.

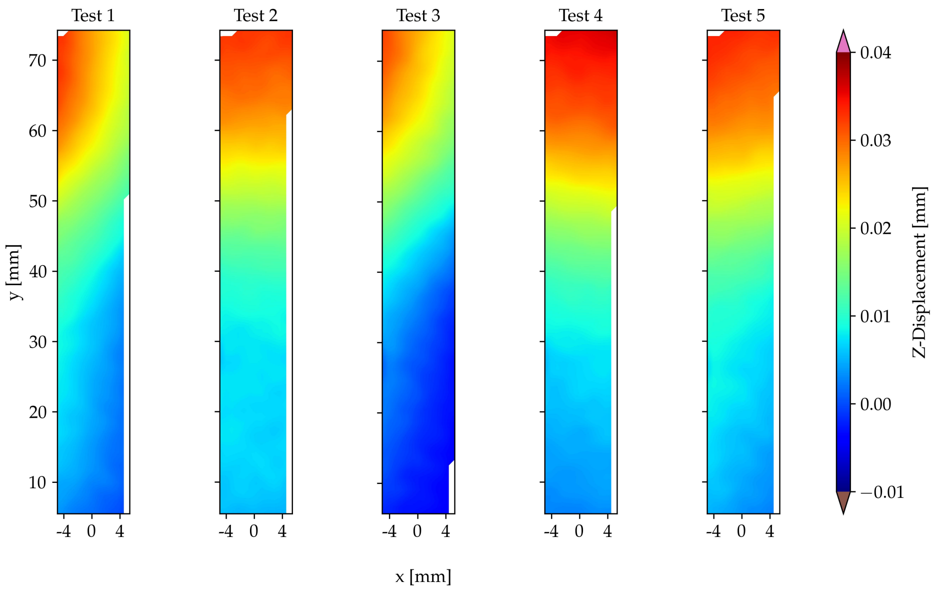

Figure 8. Out-of-plane motion, as captured by stereo-DIC, for the last image taken in the measurement.

3.2. Complex Tensile Specimen Tests

In the tests performed on the complex specimens, all three of the tests demonstrated improved accuracy in their 2D-DIC strain measurements after the application of the error compensation method. A set of contour plots was drawn up for each of the experiments, similar to the plots shown in Section 3.1. In all of the following figures, the plot labels have the same meaning as the labels used in Figure 6. For reference, the plots which follow have all been carried out for the 700th image taken during each measurement, which is a point well beyond the yield strength of the specimen material.

1. **Test 1:** A significant improvement was obtained in the accuracy of the 2D-DIC measurement in Test 1, as is evident in Figure 9. Specifically, the contour plot of the corrected 2D-DIC data approaches the contour plot of the stereo-DIC data when compared to the original (uncorrected) 2D-DIC data contour plot. A clear reduction in the magnitude of the strain error values is also present over most of the strain field in the plots of the absolute strain error before and after correction.

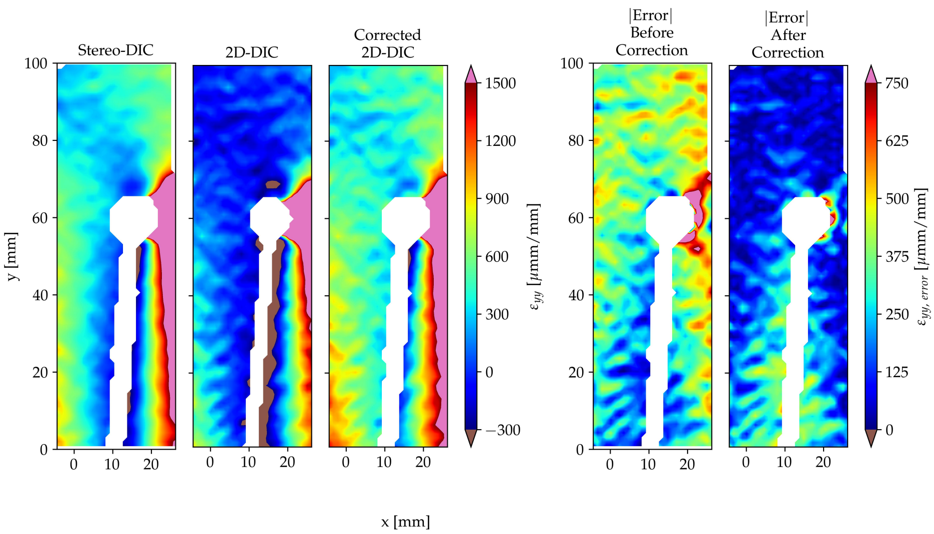

Figure 9. Contour plots of the stereo-DIC, 2D-DIC, corrected 2D-DIC and error data for strain in the y-direction for the 700th image of Test 1.

The improvement in accuracy is also shown in Figure 10 where the probability density histogram shifted to the left-hand-side of the plot and the width of the peak is reduced. This indicates that the probability density of the errors close to the experiment's 2D-DIC noise-floor both increased and became more concentrated after the error compensation method was applied.

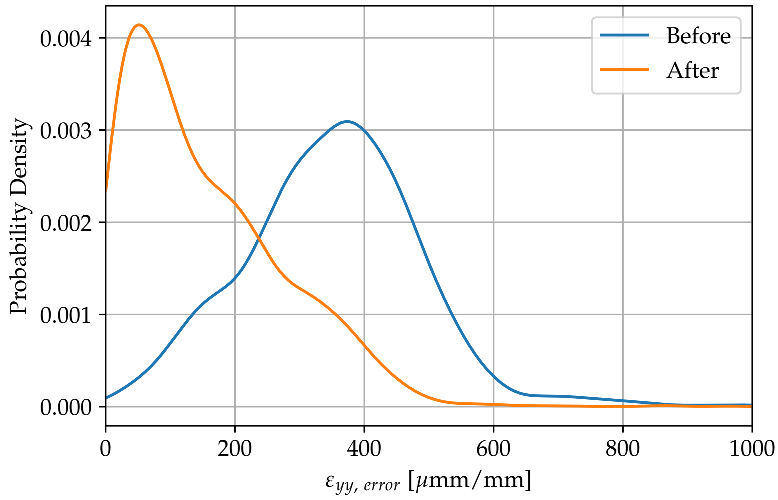

Figure 10. A histogram showing the change in the probability density of the error from the application of the error compensation method. This data is also for the 700th image of Test 1.

The line plot in Figure 11 is included here to demonstrate that the error was successfully compensated for in the entire measurement (and not only for a single image).

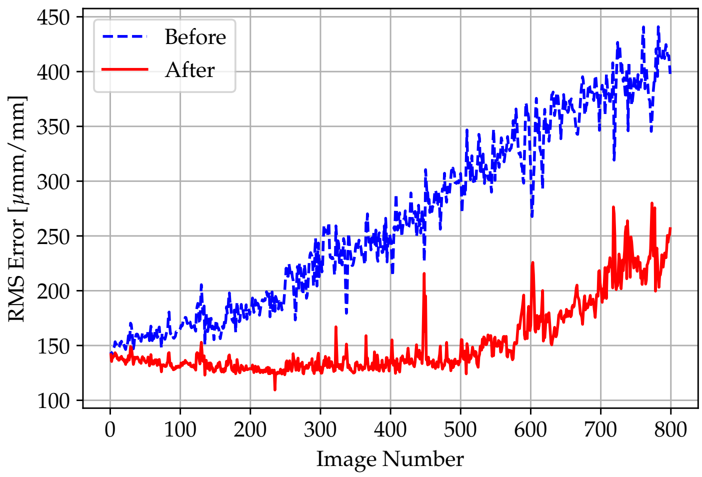

Figure 11. The RMS strain error between the stereo-DIC and 2D-DIC measurements, before and after the error compensation was applied, for Test 1.

2. **Test 2:** Similarly, the 2D-DIC measurement accuracy of Test 2 substantially improved because of the error compensation method, which can be seen in Figure 12. The appearance of the corrected 2D-DIC contour plot again approaches that of the stereo-DIC contour plot in comparison to the contour plot of the uncorrected 2D-DIC data. An improvement in accuracy is seen in how the magnitude of the majority of the strain error values also decreased between the contour plots of the |Error| Before and After Correction.

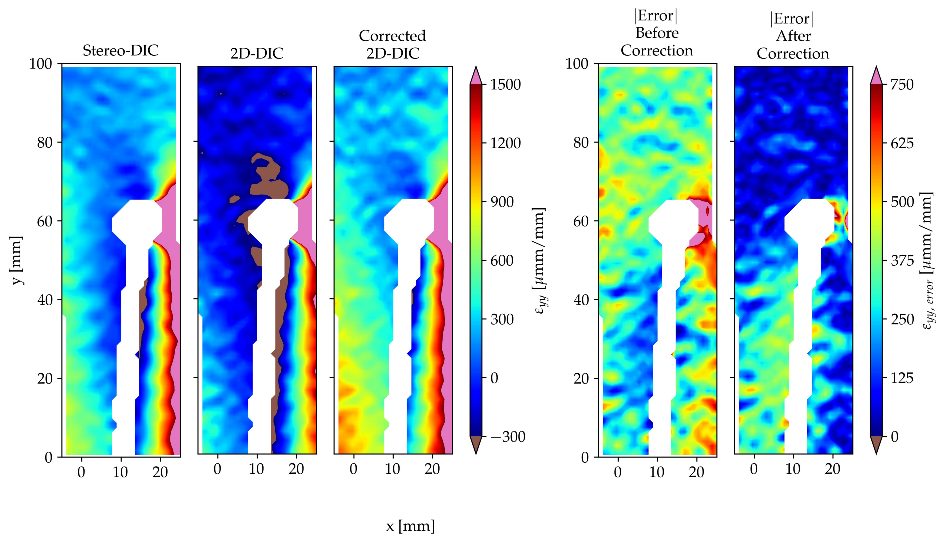

Figure 12. Contour plots of the stereo-DIC, 2D-DIC, corrected 2D-DIC and error data for the 700th image of Test 2.

Figure 13 also shows the improved accuracy of the 2D-DIC data as a result of the error compensation method, in the same way that Figure 10 does.

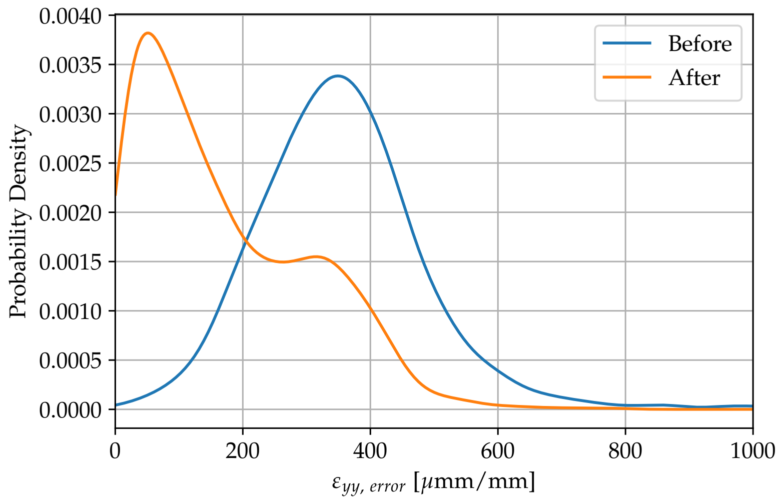

Figure 13. A histogram showing the change in the probability density of the error from the application of the error compensation method. This data is also for the 700th image of Test 2.

As before, the line plot in Figure 14 is presented here as it shows that the strain error was compensated for in the entire DIC measurement.

3. **Test 3:** Unlike in Tests 1 and 2, the error compensation method did not produce a considerable improvement in the 2D-DIC measurement accuracy. The strain error was indeed reduced in Test 3, as shown in Figure 15, although this reduction is relatively minor compared to that of Tests 1 and 2. Both in the case of the appearance of the 2D-DIC contour plots (before and after correction), and in the case of the decrease in the magnitude of the strain error values in the |Error| plots (before and after correction), a relatively small improvement in accuracy is still noticeable here.

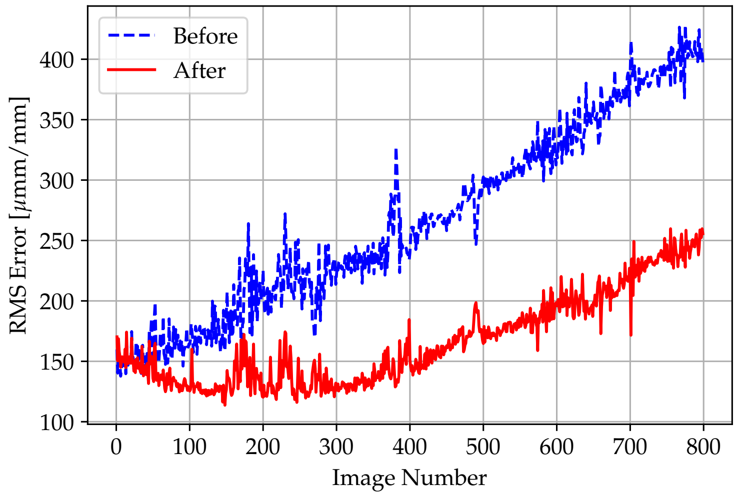

Figure 14. The RMS strain error between the stereo-DIC and 2D-DIC measurements, before and after the error compensation was applied, for Test 2.

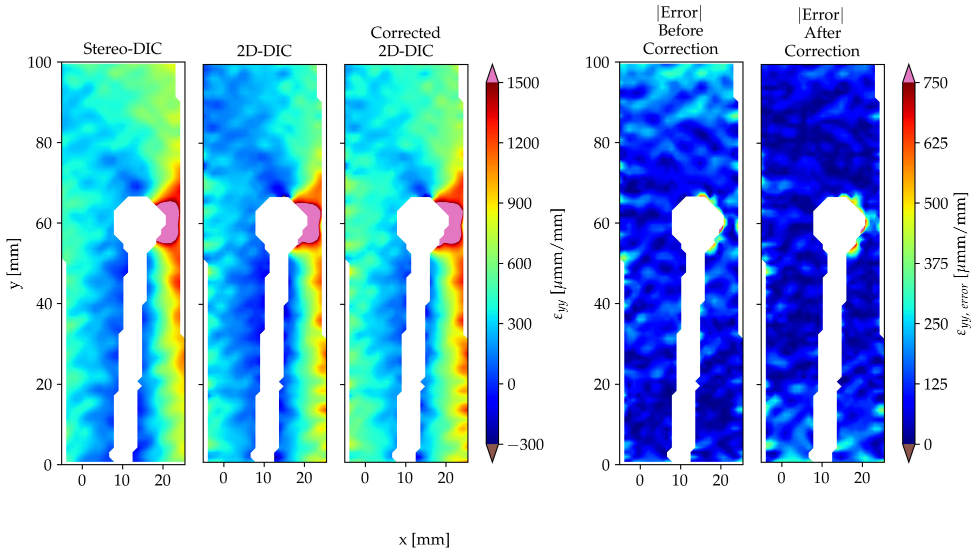

Figure 15. Contour plots of the stereo-DIC, 2D-DIC, corrected 2D-DIC and error data for the 700th image of Test 3.

Correspondingly, the probability density histogram, shown in Figure 16, also did not show a large improvement in the 2D-DIC measurement accuracy. Even though the histogram's left-hand-side shift was not as drastic as in Test 1 and 2, the peak of the histogram for Test 3 clearly increased and moved closer to the 2D-DIC noise-floor. This shows that the strain errors were indeed reduced.

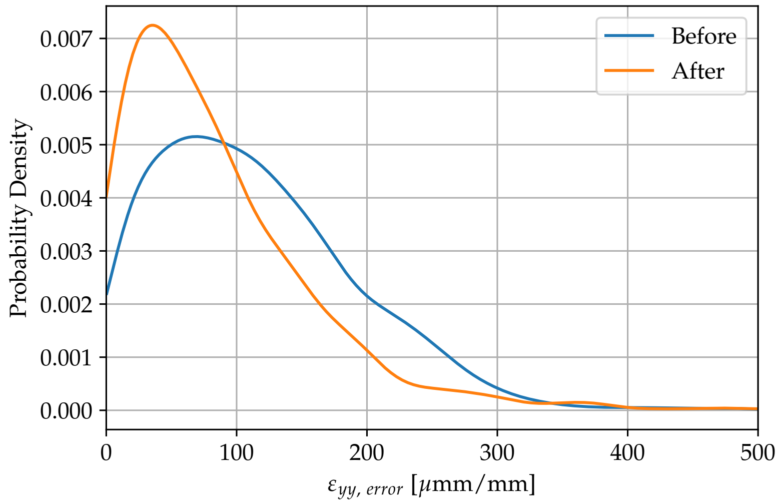

Figure 16. A histogram showing the change in the probability density of the error from the application of the error compensation method. This data is also for the 700th image of Test 3.

Although it is not as clear here as it was in Test 1 and 2, Figure 17 shows that a slight improvement in 2D-DIC accuracy was obtained over the entire measurement.

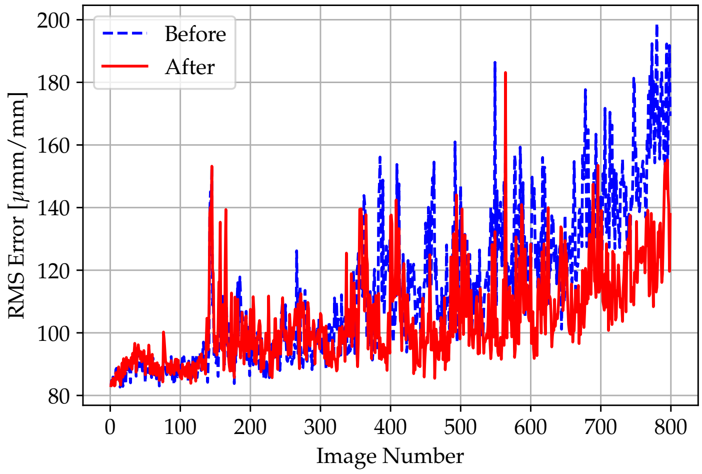

Figure 17. The RMS strain error between the stereo-DIC and 2D-DIC measurements, before and after the error compensation was applied, for Test 3.

The difference in how the accuracy improved between Tests 1 and 2, and Test 3, can be attributed to how Test 3 had a lower strain error, before the error compensation method was applied, than Tests 1 and 2. As shown in Figure 16, the error before correction is already close to the noise-floor, so a minor improvement (until the noise-floor) is to be expected for Test 3. When one considers the out-of-plane motion for all three plots, which is shown in Figure 18, then it can be seen that Test 3 experienced significantly less out-of-plane motion than Tests 1 and 2. The amount of out-of-plane motion would cause a proportionally large strain error in the 2D-DIC data, and so the strain error in Test 3 would be lower than Tests 1 and 2. Since the proposed error compensation method corrects for strain errors from out-of-plane motion, the compensation method is less successful when the out-of-plane motion is lower, as in Test 3. The lower amount of out-of-plane motion in Test 3 also explains why the error before correction is significantly lower than in the other two tests, as this would result in less of a strain error than in the other two tests, as shown in Figure 17. When considering the contour plots of the stereo-DIC and (uncorrected) 2D-DIC data in Figure 15, it can be seen that the 2D-DIC performed a relatively accurate measurement without any correction, which further explains why the error compensation method did not lead to a significant improvement in accuracy.

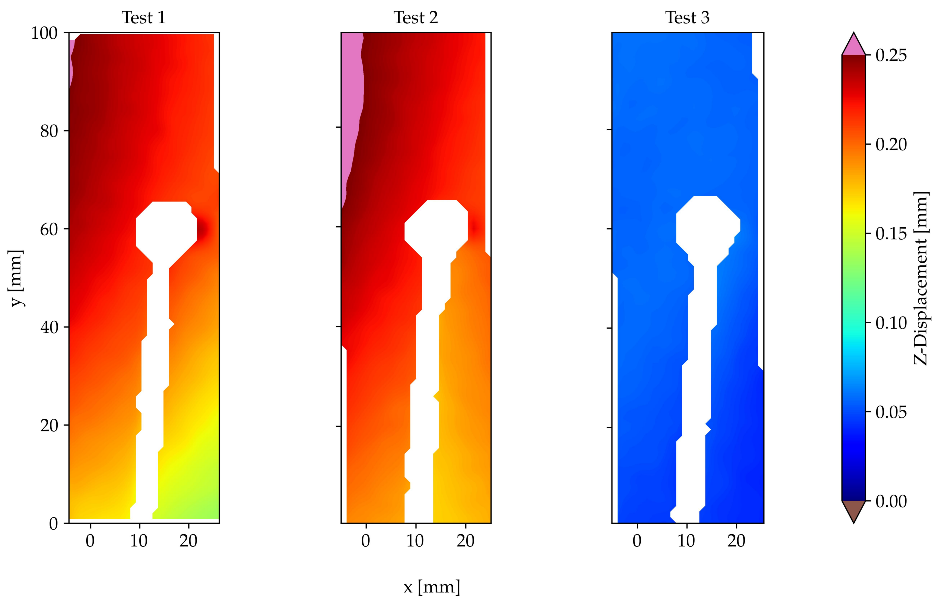

Figure 18. Out-of-plane motion, as captured by stereo-DIC, for the 700th image taken in the measurement.

4. Discussion

As the results in Section 3 demonstrate, the proposed strain-gauge-based error compensation method successfully improves the accuracy of 2D-DIC data. It is, therefore, able to serve as a compensation method for strain errors from out-of-plane motion in 2D-DIC measurement data. Compared to other compensation methods which correct for out-of-plane motion, this method is a relatively simple compensation method to apply and is also relatively low-cost in nature (if a low-cost bridge amplifier is used). Even though the strain-gauge-based error compensation method is a less expensive compensation method than using a bilateral telecentric lens, it is not as easy to apply as using a bilateral telecentric lens is [13]. Similarly, even though the hardware and software requirements are simpler for the strain-gauge-based error compensation method than for the Region of Compensation method, it has the benefit of correcting for errors in both strain and displacement measurements and correcting for errors both from lens distortions and out-of-plane motion [11]. While the application of the method means that 2D-DIC loses its non-contact measurement feature (due to strain gauges being applied to the test specimen), this is also a drawback of other methods, such as the Region of Compensation (ROC) method. Moreover, the strain-gauge-based error compensation method uses a well-understood measurement instrument commonly found in experimental mechanics laboratories in the form of strain gauges for error compensation. The ROC method uses a custom-made, single-purpose compensation panel for correction though, which gives the proposed compensation method an advantage over the ROC method. The presence of the strain gauges actually has an advantage over using a region of compensation to correct for errors as the strain gauges provide highly accurate strain readings at discrete locations (which the ROC method does not). The error compensation method can serve as a relatively low-cost tool to improve 2D-DIC accuracy and to make 2D-DIC a more viable measurement tool, therefore making it a more attractive alternative to stereo-DIC when it is not practically viable or available.

The error compensation method showed in all of the test cases that it either led to an improvement in accuracy or that it kept the measurement accuracy relatively constant, although the amount of improvement in 2D-DIC measurement accuracy from the compensation method is linked to the amount of error from out-of-plane motion in the measurement. Specifically, when there is relatively little error from out-of-plane motion in a measurement, as was the case in the tests from Section 3.1, then the there is little error which the error compensation method is able correct for. In the case of the tests from Section 3.2, there was a significant amount of out-of-plane motion, and, therefore, a significant amount of error to correct for, which correspondingly led to a greater improvement in the strain measurement accuracy (compared to the improvement for the simple specimen tests). One can, thus, safely apply the error compensation method without knowing how large the error from out-of-plane motion is. A significant drawback of the compensation method is the increased hardware and software complexity that comes from using the method in a measurement setup, for example due to the application of strain gauges to the specimen, and having to use a data acquisition system and using its associated software. However, the application and data acquisition of the strain gauges is well understood in most experimental strain measurement contexts and is, therefore, easily integrated with 2D-DIC measurements using this method. Some limitations of the error compensation method to take note of are that it can only be applied in test cases where strain gauges can be applied to the test specimen, and that as of yet, the compensation method has only been applied to test cases with planar specimens. Potential future work is to apply the strain-gauge-based error compensation method to non-planar specimens to determine if the method can also be used in other test cases.

5. Conclusions

A strain-gauge-based error compensation method which corrects for strain errors from out-of-plane motions in 2D-DIC measurements in planar specimens was proposed. After considering the theoretical strain errors from out-of-plane translation and rotation in a 2D-DIC measurement, a single equation was obtained which describes the total strain error from out-of-plane motion in a 2D-DIC data field. Strain gauges were thus used to find the strain errors at a set of locations on the full-field 2D-DIC data, and these strain errors were then used to solve for unknown coefficients in the simplified strain error equation. With these found, the strain error from out-of-plane motion in the 2D-DIC data could be determined and then removed from the data to produce a more accurate 2D-DIC measurement. The functionality of this error compensation method was verified in two sets of experiments, each of which was carried out on a different dog-bone specimen geometry. The tests performed on a standard, simple specimen geometry the error compensation method produced minor improvements in the measurement accuracy simply because the measurements had relatively little error to correct. Of the three test performed on the complex, slotted specimen geometry, all three showed that the application of the strain-gauge-based error compensation method leads to more accurate 2D-DIC measurements provided the errors resulting from out-of-plane motion exceeds the strain noise-floor. By using the strain-gauge-based error compensation method, the accuracy of 2D-DIC measurements can be improved in a relatively simple and low-cost manner. This makes 2D-DIC a more reliable non-contact, full-field deformation measurement tool, and allows it to serve as an alternative for measuring surface deformations when stereo-DIC is perhaps not an option.

Author Contributions: Conceptualization, C.-H.V., G.V. and M.N.; methodology, C.-H.V., G.V. and M.N.; software, C.-H.V.; formal analysis, C.-H.V.; investigation, C.-H.V.; resources, G.V. and M.N.; data curation, C.-H.V.; writing—original draft preparation, C.-H.V.; writing—review and editing, C.-H.V., G.V. and M.N.; visualization, C.-H.V.; supervision, G.V. and M.N.; project administration, G.V. and M.N.; funding acquisition, G.V. All authors have read and agreed to the published version of the manuscript.

Funding: This research received no external funding.

Data Availability Statement: The data from this work can be obtained at request from the author.

Conflicts of Interest: The authors declare no conflict of interest.

Abbreviations

The following abbreviations are used in this manuscript:

DIC	Digital Image Correlation
2D	Two-Dimensional
3D	Three-Dimensional
OPM	Out-of-Plane Motion
SG	Strain Gauge
VSG	Virtual Strain Gauge
RMS	Root-Mean-Square
ROC	Region of Compensation

References

1. Peters, W.H.; Ranson, W.F. Digital Imaging Techniques In Experimental Stress Analysis. *Opt. Eng.* **1982**, *21*, 213427. [CrossRef]
2. Libertiaux, V.; Pascon, F.; Cescotto, S. Experimental verification of brain tissue incompressibility using digital image correlation. *J. Mech. Behav. Biomed. Mater.* **2011**, *4*, 1177–1185. [CrossRef] [PubMed]
3. Van Rooyen, M.; Becker, T.; Westraadt, J.; Marx, G. Creep Damage Assessment of Ex-Service 12% Cr Power Plant Steel Using Digital Image Correlation and Quantitative Microstructural Evaluation. *Materials* **2019**, *12*, 3106. [CrossRef] [PubMed]
4. Walley, J.L.; Wheeler, R.; Uchic, M.D.; Mills, M.J. In-Situ Mechanical Testing for Characterizing Strain Localization During Deformation at Elevated Temperatures. *Exp. Mech.* **2012**, *52*, 405–416. [CrossRef]
5. Pan, B.; Qian, K.; Xie, H.; Asundi, A. Two-dimensional digital image correlation for in-plane displacement and strain measurement: A review. *Meas. Sci. Technol.* **2009**, *20*, 062001. [CrossRef]
6. Hijazi, A.L. A Novel Approach for the Determination of Surface Tilt Angles in Two-Dimensional Digital Image Correlation Experiments. *Exp. Mech.* **2020**, *60*, 267–282. [CrossRef]
7. Pan, B.; Yu, L.; Wu, D.; Tang, L. Systematic errors in two-dimensional digital image correlation due to lens distortion. *Opt. Lasers Eng.* **2013**, *51*, 140–147. [CrossRef]
8. Sutton, M.A.; Yan, J.H.; Tiwari, V.; Schreier, H.W.; Orteu, J.J. The effect of out-of-plane motion on 2D and 3D digital image correlation measurements. *Opt. Lasers Eng.* **2008**, *46*, 746–757. [CrossRef]
9. Pan, B.; Yu, L.; Wu, D. High-accuracy 2D digital image correlation measurements using low-cost imaging lenses: Implementation of a generalized compensation method. *Meas. Sci. Technol.* **2014**, *25*, 025001. [CrossRef]
10. Wittevrongel, L.; Badaloni, M.; Balcaen, R.; Lava, P.; Debruyne, D. Evaluation of Methodologies for Compensation of Out of Plane Motions in a 2D Digital Image Correlation Setup. *Strain* **2015**, *51*, 357–369. [CrossRef]
11. Xu, X.; Zhang, Q.; Su, Y.; Cai, Y.; Xue, W.; Gao, Z.; Xue, Y.; Lv, Z.; Fu, S. High-Accuracy, High-Efficiency Compensation Method in Two-Dimensional Digital Image Correlation. *Exp. Mech.* **2017**, *57*, 831–846. [CrossRef]
12. Lava, P.; Coppieters, S.; Wang, Y.; Houtte, P.V.; Debruyne, D. Error estimation in measuring strain fields with DIC on planar sheet metal specimens with a non-perpendicular camera alignment. *Opt. Lasers Eng.* **2011**, *49*, 57–65. [CrossRef]
13. Pan, B.; Yu, L.; Wu, D. High-Accuracy 2D Digital Image Correlation Measurements with Bilateral Telecentric Lenses: Error Analysis and Experimental Verification. *Exp. Mech.* **2013**, *53*, 1719–1733. [CrossRef]
14. Jähne, B. *Practical Handbook on Image Processing for Scientific and Technical Applications*, 2nd ed.; CRC Press: Boca Raton, FL, USA, 2004.
15. *ASTM E8/E8M*; Standard Test Methods for Tension Testing of Metallic Materials. ASTM International: West Conshohocken, PA, USA, 2021.